iJRASET
International Journal For Research in Applied Science and Engineering Technology

INTERNATIONAL JOURNAL FOR RESEARCH

IN APPLIED SCIENCE & ENGINEERING TECHNOLOGY

Volume: 9 **Issue:** VI **Month of publication:** June 2021

DOI: https://doi.org/10.22214/ijraset.2021.35928

www.ijraset.com

Call: 08813907089 | E-mail ID: ijraset@gmail.com

International Journal for Research in Applied Science & Engineering Technology (IJRASET)
ISSN: 2321-9653; IC Value: 45.98; SJ Impact Factor: 7.429
Volume 9 Issue VI June 2021- Available at www.ijraset.com

A Preliminary Study of Oxygen Transport from Capillary to Tissue using Finite Difference Method

Ritesh Singh Dangwal
Saroj Institute of Technology and Management, India

Abstract: ***In this study, Finite Difference Method is used to examine oxygen transport from blood capillary to tissue. Tissue is modelled as porous media and oxygen rich blood is transported throughout the tissue from the blood vessel by advection and diffusion. Uniform consumption by tissue is considered for simplicity. Steady state flow patterns and concentration contours are discussed. A simplistic 2-D model was created after reviewing the literature. The model considers interlinkage of capillaries. Stream Function-Vorticity formulation coupled with advection-diffusion equation are solved simultaneously to evaluate velocities and concentration values in the domain. This report focuses on the how various parameters affect flow and mass transfer inside a porous media. Effect of various non dimensional parameters like Darcy number and non-dimensional absorption coefficient are discussed.***

I. INTRODUCTION

The study of oxygen transport to tissue is complicated because of heterogeneity in the distribution of capillaries throughout the tissue. The first theoretical model for the study of oxygen transport through the tissue was proposed by Krogh and Erlang [1]. It was a very basic model and several assumptions were used like one dimensional study state oxygen transport, constant and uniform oxygen consumption by tissue. Many of their assumptions were later followed in the works of many researchers.

Later it was found out that oxygen consumption was not constant and first order kinetics was used by Michaelis-Menten [2] in their model. Their model did not keep oxygen consumption strictly constant but gave a reasonable approximation to the actual behavior and is more convenient computationally. Axial convection in tissues is more important than axial diffusion inside flowing micro-vessels. Lagerlund and Low [3] used a Krogh-type model with axial diffusion and Michaelis-Menten consumption to study steady-state oxygen transport in rat peripheral nerve tissue. They solved the steady-state equations using a finite-difference method and found better agreement with experiment for reduced oxygen supply than in a model with constant oxygen consumption and no axial diffusion. The subsequent models developed after the above models considered multi vessel transport models such as parallel capillary model and capillary network models. The effects of heterogeneities in capillary spacing, oxygen supply and flow direction requires more sophisticated models. The model by Popel [4] uses a slab of tissue bounded by plane surfaces and the capillaries are parallel to the surface of the tissue and form a square lattice. He showed how the diffusive interaction between the surface and the tissue affects the oxygen distribution in the surface layers of tissue and for convenience, the results were presented in terms of dimensionless coordinates. He solved the mathematical model numerically using a computer program by implementing a finite-element scheme with triangular elements. The numerical scheme was tested on many geometries, including the simplest case of identical capillaries forming a square lattice as well as more complex geometries.

A realistic geometric model for the three-dimensional capillary network geometry is used as a framework for studying the transport and consumption of oxygen in cardiac tissue by Daniel A. Beard and James B. Bassingthwaighte [5]. They explored the steady-state oxygen transport and consumption in the tissue using a mathematical model which accounts for advection in the vascular network and Michaelis–Menten consumption in the parenchymal tissue. The hemodynamic problem for flow throughout the network was solved to evaluate the advection velocity field. A set of coupled nonlinear elliptic equations was used to describe the resulting system, which was solved using a finite-difference numerical approximation. The coupled advection and diffusion in the three-dimensional system was found out to enhance the dispersion of oxygen in the tissue compared to the predictions of simplified axially distributed models, and that no “lethal corner,” or oxygen-deprived region occurs for physiologically reasonable values for flow and consumption. Khalil M. Khanafer and Ali J. Chamkha [6] formulated Volume averaged equations (mass conservation, linear momentum conservation and thermal energy conservation) governing unsteady, laminar, mixed convection flow in an enclosure filled with a Darcian fluid and saturated uniform porous medium in the presence of internal heat generation. In their algorithm, alternating direct implicit (ADI) procedure was used along with the successive grid refinement scheme which were respectively implemented in the spatial and temporal environments to accelerate the convergence of the solution towards steady state.

©IJRASET: All Rights are Reserved

International Journal for Research in Applied Science & Engineering Technology (IJRASET)
ISSN: 2321-9653; IC Value: 45.98; SJ Impact Factor: 7.429
Volume 9 Issue VI June 2021- Available at www.ijraset.com

II. FORMULATION OF THE PROBLEM

A schematic of a two dimensional tissue with blood vessels is shown in Fig 2.1 below. The figure shows the physical domain of our problem. It depicts an artery coming from left and it gets divided in two capillaries (red in figure) which runs around the tissue i.e., porous media (yellow in figure) and then the capillaries unite to form a vein. Since the physical domain is symmetric about centerline (dashed in figure 2.1), so we can solve only for the half domain.

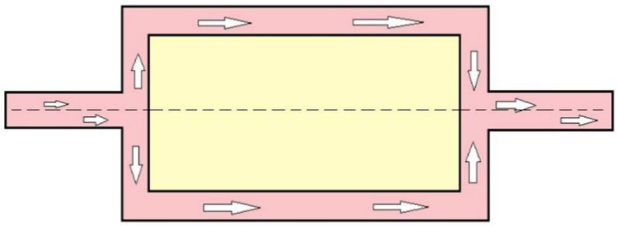

Figure 2.1 Schematic of Physical Domain

Figure 2.2 shows the computational domain which is the upper half of the physical domain. All the boundaries conditions are marked in figure which are Dirichlet boundary condition on three sides (left, top and right) and Neumann boundary condition on the bottom side. This computational domain has been used for validation of our code only.

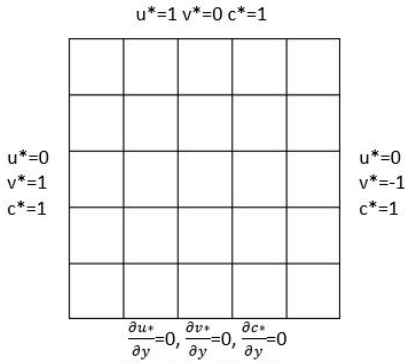

Figure 1.2 Schematic of Computational Domain

A. Governing Equations

Continuity: $$\frac{\partial u}{\partial x}+\frac{\partial v}{\partial y}=0$$

x-Momentum: $$\frac{\partial u}{\partial t}+u\frac{\partial u}{\partial x}+v\frac{\partial u}{\partial y}=-\frac{1}{\rho_o}\frac{\partial p}{\partial x}+\Phi\vartheta^{eff}\left(\frac{\partial^2 u}{\partial x^2}+\frac{\partial^2 u}{\partial y^2}\right)-\Phi\frac{\mu u}{\rho_o \kappa}$$

y-Momentum: $$\frac{\partial u}{\partial t}+u\frac{\partial u}{\partial x}+v\frac{\partial u}{\partial y}=-\frac{1}{\rho_o}\frac{\partial p}{\partial x}+\Phi\vartheta^{eff}\left(\frac{\partial^2 u}{\partial x^2}+\frac{\partial^2 u}{\partial y^2}\right)-\Phi\frac{\mu u}{\rho_o \kappa}$$

Concentration: $$\frac{\partial c}{\partial t}=D\nabla^2 c-\frac{\vec{v}}{\Phi}.\nabla c-\beta c$$

where,

u: intrinsic volume averaged velocity
c: mass concentration
Φ: porosity
κ : permeability
D: mass diffusivity
β : adsorption

©IJRASET: All Rights are Reserved

B. Solution Methodology

Finite difference discretization method

Stream function and Vorticity formulation with Finite difference discretization method has been used to solve the above equations and since the concentration-diffusion equation is also coupled, therefore it is solved simultaneously with stream function and vorticity equation as follows: -

$$-\xi = \frac{\partial^2\psi}{\partial x^2} + \frac{\partial^2\psi}{\partial y^2}$$

$$\frac{\partial\xi}{\partial t} + u\frac{\partial\xi}{\partial x} + v\frac{\partial\xi}{\partial y} = \Phi\vartheta^{eff}\left(\frac{\partial^2\xi}{\partial x^2} + \frac{\partial^2\xi}{\partial y^2}\right) - \Phi\frac{\mu\xi}{\rho_o\kappa}$$

$$\frac{\partial c}{\partial t} + \frac{\vec{v}}{\Phi}.\nabla c = D\nabla^2 c - \beta c$$

where,

Vorticity , $\xi = \frac{\partial v}{\partial x} - \frac{\partial u}{\partial y}$ Stream function, ψ: $u = \frac{\partial\psi}{\partial y}$, v= $-\frac{\partial\psi}{\partial x}$

The above equations are converted to non-dimensional form using first order upwinding and implicit discretization schemes. Successive substitution formulas are developed for all three equations for getting diagonal dominance and applying Gauss-Seidel method.

Stream function equation in non-dimensional form: -

$$\frac{\partial\psi}{\partial t} = \xi + \frac{1}{G}\left(\frac{\partial^2\psi}{\partial x^2} + \frac{\partial^2\psi}{\partial y^2}\right)$$

Where G = non-dimensional constant for false transience in stream function equation

Discretized form of the stream function equation is: -

$$\frac{\psi^{n+1}(i,j)-\psi^n(i,j)}{dt} = \xi^{n+1}(i,j) + \frac{\psi^{n+1}(i+1,j)-2\psi^{n+1}(i,j)+\psi^{n+1}(i-1,j)}{G*(dx)^2} + \frac{\psi^{n+1}(i,j+1)-2\psi^{n+1}(i,j)+\psi^{n+1}(i,j-1)}{G*(dy)^2}$$

Rearranging the above equation

$$a_e\psi^{n+1}(i+1,j) + a_w\psi^{n+1}(i-1,j) + a_n\psi^{n+1}(i,j+1) + a_s\psi^{n+1}(i,j-1) + a_p\psi^{n+1}(i,j) = \psi^n(i,j) + \xi^{n+1}(i,j)$$

$$a_e\psi_e + a_w\psi_w + a_n\psi_n + a_s\psi_s + a_p\psi_p = m + q$$

where m and q are the previous iteration values of stream function and vorticity respectively.

$a_e = \frac{-dt}{(dx)^2}$ $a_w = \frac{-dt}{(dx)^2}$ $a_n = \frac{-dt}{(dy)^2}$ $a_s = \frac{-dt}{(dy)^2}$

a_p= 1-$(a_e + a_w + a_n + a_s)$

The successive substitution formula for stream function is: -

$$\psi_p = \frac{-(a_e\psi_e + a_w\psi_w + a_n\psi_n + a_s\psi_s) + q + m}{a_p}$$

Vorticity equation in non-dimensional form is: -

$$\frac{\partial\xi}{\partial t} + \frac{u\partial\xi}{\partial x} + \frac{v\partial\xi}{\partial y} = \frac{1}{Re}\left(\frac{\partial^2\xi}{\partial x^2} + \frac{\partial^2\xi}{\partial y^2}\right) + \frac{\phi}{DaRe}\xi$$

©IJRASET: All Rights are Reserved

Discretized form of the vorticity equation using implicit method is: -

$$\frac{\xi^{n+1}(i,j)-\xi^{n}(i,j)}{dt}+\frac{u^{n+1}(i,j)(\xi^{n+1}(i+1,j)-\xi^{n+1}(i,j))}{dx}+\frac{v^{n+1}(i,j)(\xi^{n+1}(i,j+1)-\xi^{n+1}(i,j))}{dy}$$
$$=\frac{1}{Re}\frac{\xi^{n+1}(i+1,j)-2\xi^{n+1}(i,j)+\xi^{n+1}(i-1,j)}{dx^2}+\frac{1}{Re}\frac{\xi^{n+1}(i,j+1)-2\xi^{n+1}(i,j)+\xi^{n+1}(i,j-1)}{dy^2}$$
$$+\frac{\phi}{DaRe}\xi^{n+1}(i,j)$$

Rearranging the above equation, we get

$$a_{e1}\xi^{n+1}(i+1,j)+a_{w1}\xi^{n+1}(i-1,j)+a_{n1}\xi^{n+1}(i,j+1)+a_{s1}\xi^{n+1}(i,j-1)+a_{p1}\xi^{n+1}(i,j)=\xi^{n}(i,j)$$

$$a_{e1}\xi_e+a_{w1}\xi_w+a_{n1}\xi_n+a_{s1}\xi_s+a_{p1}\xi_p=\mathrm{q}$$

$$a_{e1}=\left|\frac{u(i,j)*dt*ie}{dx}\right|+\left|\frac{\phi*dt}{Re*(dx)^2}\right| \qquad a_{w1}=\left|\frac{u(i,j)*dt*iw}{dx}\right|+\left|\frac{\phi*dt}{Re*(dx)^2}\right|$$

$$a_{n1}=\left|\frac{v(i,j)*dt*in}{dy}\right|+\left|\frac{\phi*dt}{Re*(dy)^2}\right| \qquad a_{s1}=\left|\frac{v(i,j)*dt*is}{dy}\right|+\left|\frac{\phi*dt}{Re*(dy)^2}\right|$$

$$a_{p1}=1-(a_{e1}+a_{w1}+a_{n1}+a_{s1})+\frac{\phi*dt}{Re*Da}$$

Now, using first order up-winding

If u>0, iw =1, ie=0

If u<0, iw =0, ie=1

If v>0, in =0, is=1

If v<0, in=1, is=0

The successive substitution formula for stream function is: -

$$\xi_p=\frac{-(a_{e1}\xi_e+a_{w1}\xi_w+a_{n1}\xi_n+a_{s1}\xi_s)+q}{a_{p1}}$$

Concentration –Diffusion equation in non-dimensional form is: -

$$\frac{\partial c}{\partial t}+\phi^{-1}\left(\frac{u\partial c}{\partial x}+\frac{v\partial c}{\partial y}\right)=A\left(\frac{\partial^2 c}{\partial x^2}+\frac{\partial^2 c}{\partial y^2}\right)-Bc$$

Discretized form of the concentration-diffusion equation using implicit method is:

$$-\frac{c^{n+1}(i,j)-c^{n}(i,j)}{dt}+\frac{u^{n+1}(i,j)(c^{n+1}(i+1,j)-c^{n+1}(i,j))}{\phi*dx}+\frac{v^{n+1}(i,j)(c^{n+1}(i,j+1)-c^{n+1}(i,j))}{\phi*dy}=A\frac{c^{n+1}(i+1,j)-2c^{n+1}(i,j)+c^{n+1}(i-1,j)}{dx^2}+$$
$$A\frac{c^{n+1}(i,j+1)-2c^{n+1}(i,j)+c^{n+1}(i,j-1)}{dy^2}-Bc^{n+1}(i,j)$$

Rearranging the above equation, we get

$$a_{e1}c^{n+1}(i+1,j)+a_{w1}c^{n+1}(i-1,j)+a_{n1}c^{n+1}(i,j+1)+a_{s1}c^{n+1}(i,j-1)+a_{p1}c^{n+1}(i,j)=c^{n}(i,j)$$

$$a_{e1}c_e+a_{w1}c_w+a_{n1}c_n+a_{s1}c_s+a_{p1}c_p=\mathrm{c_old}$$

$$a_{e1}=\left|\frac{u(i,j)*dt*ie}{\phi*dx}\right|+\left|\frac{A*dt}{(dx)^2}\right| \qquad a_{w1}=\left|\frac{u(i,j)*dt*iw}{\phi*dx}\right|+\left|\frac{A*dt}{(dx)^2}\right|$$

©IJRASET: All Rights are Reserved

$a_{n1}=\left|\frac{v(i,j)*dt*in}{\phi*dy}\right|+\left|\frac{A*dt}{(dy)^2}\right|$ $a_{s1}=\left|\frac{v(i,j)*dt*is}{\phi*dy}\right|+\left|\frac{A*dt}{(dy)^2}\right|$

$a_{p1}= 1-(a_{e1}+a_{w1}+a_{n1}+a_{s1})+dt*B$

Now, using first order up-winding

If u>0, iw =1, ie=0

If u<0, iw =0, ie=1

If v>0, in =0, is=1

If v<0, in=1, is=0

The successive substitution formula for stream function is: -

$$c_p=\frac{-(a_{e1}c_e+a_{w1}c_w+a_{n1}c_n+a_{s1}c_s)+\text{c_old}}{a_{p1}}$$

III. VALIDATION

The code used for the simulations is based on finite difference discretization method and it has been written in MATLAB. The code has been validated with the published results including results from both clear and porous media.

A. Case 1: Clear Media

The code for the clear media has been validated with the Ghia, Ghia and Shin [7]. The lid driven cavity case for clear media was solved for 129 grid points in each direction and Reynolds number is taken as 10. The figure 3.1 below shows the computational domain along with boundary conditions for the validation case. The result for validation are shown in Table 3.1.

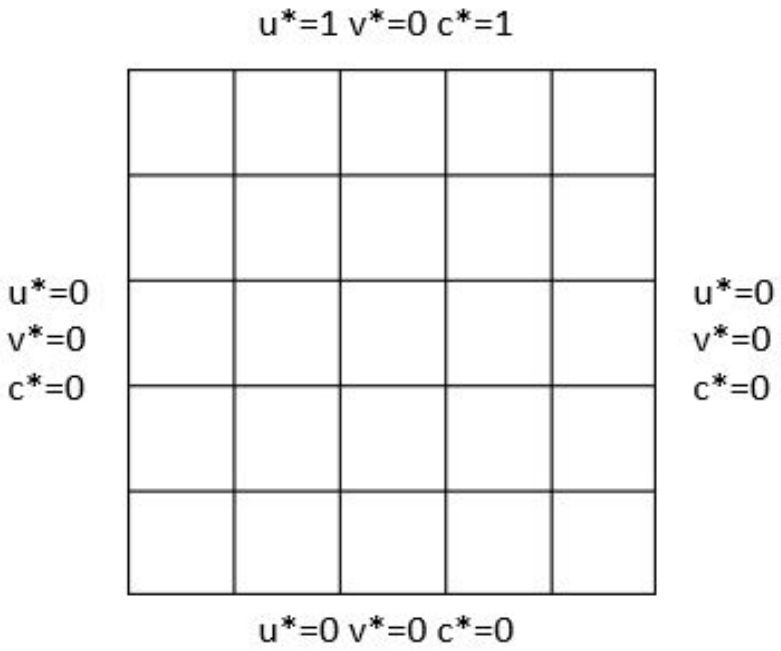

Figure 3.1 Validation case 1 (Clear Media) Computational domain

©IJRASET: All Rights are Reserved

Table 3.1 Validation results for clear media

y-grid	u	u1	%error
129	1	1	0
126	0.84123	0.843034	0.214468
125	0.78871	0.791036	0.294857
124	0.73722	0.740026	0.380584
123	0.68717	0.690402	0.47037
110	0.23151	0.23537	1.667169
95	0.00332	0.003363	1.285039
80	-0.13641	-0.13904	1.928317
65	-0.20581	-0.2086	1.358036
59	-0.2109	-0.21319	1.083893
37	-0.15662	-0.15668	0.035387
23	-0.1015	-0.10104	0.454052
14	-0.06434	-0.06397	0.582082
10	-0.04775	-0.0463	3.027128
9	-0.04192	-0.04168	0.561571
8	-0.03717	-0.03696	0.558146
1	0	0	0

The maximum error found was 3% and it can be considered to be within acceptable range.

B. Case 2: Porous Media

The code for the porous media has been validated with the Guo and Zhao [8]. The computational domain for porous media is same as clear media domain. The lid driven cavity case for clear media was solved for 129 grid points in each direction and Reynolds number is taken as 10. Porosity and Darcy number are taken as 0.1 and 0.01 respectively. The u-velocity at x-grid point number 65 for different values of y-grid points (that is the velocity at the mid-plane) was plotted. The plot was matched with Guo and Zhao [8] for same parameters. In figure 3.2 it is easily seen that our plot matches closely. We can observe that in figure 3.3, the streamline contours also show a close fit with the results from Guo et al.

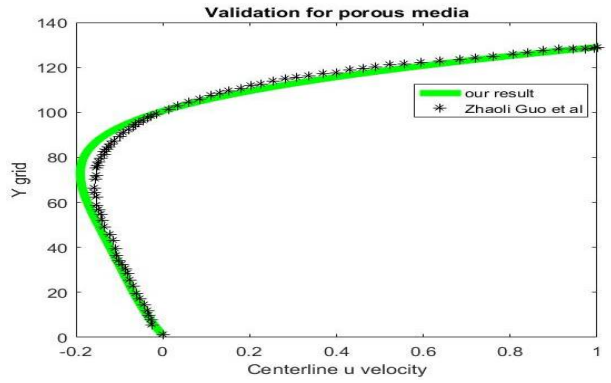

Figure 3.2 Lattice Boltzmann model for incompressible flows through porous media-Zhaoli Guo and T. S. Zhao

©IJRASET: All Rights are Reserved

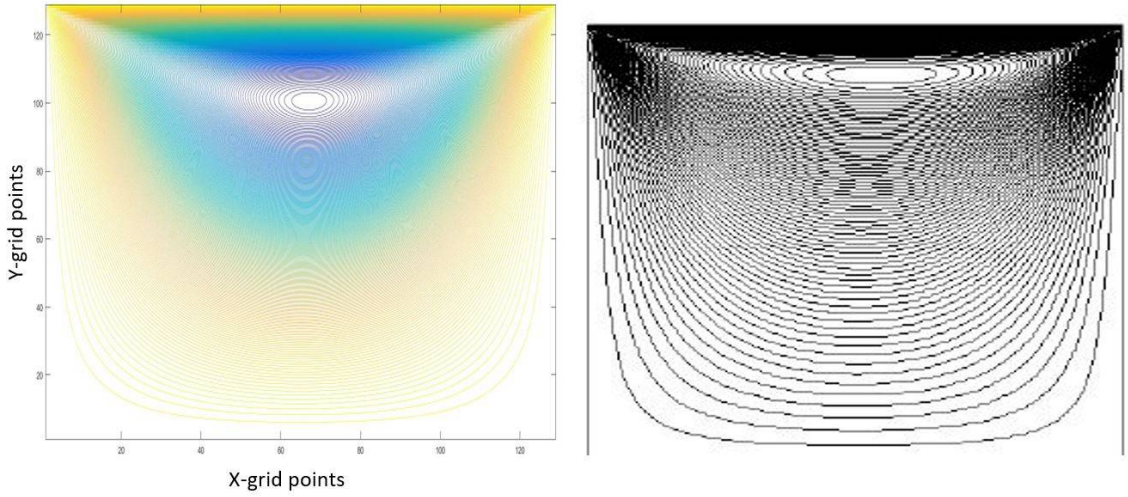

Fig. Our streamline contours in porous media (Reynolds number=10 ,Darcy number = 0.01)

Fig. Zhaoli Guo et. al. streamline contours in porous media (Reynolds number=10 Darcy number = 0.01)

Figure 3.3 Stream line contours

IV. RESULTS AND DISCUSSIONS

Three cases are run with the validated code as follows:

A. Lid Driven Flow

Lid driven cavity problem for porous media was solved with porosity, Darcy number and Reynolds number taken as 0.75, 0.1 and 10 respectively. The streamlines were plotted and an interesting property of porous media can be seen in figure 4.1 (a). Porous media does not allow vortex to grow and thus reduces velocity fluctuations. For the case of Lid driven cavity flow in clear media, it is known that three vortices (primary, secondary and tertiary) are formed. Primary vortex is formed at the top causing the major recirculation in the domain. Secondary and tertiary vortex are formed in the bottom right and left side respectively. In figure 4.1 (a), it is seen that secondary and tertiary vortex were not able to form because of the porous media. Non-dimensional concentration contour was also plotted in figure 4.1 (b). Oxygen is diffused from the top plane only and is consumed uniformly by the whole domain. Oxygen is diffused from the walls to the centre of the domain, so the maximum value of concentration is found at the walls and the minimum value of concentration is found at the centre of the domain.

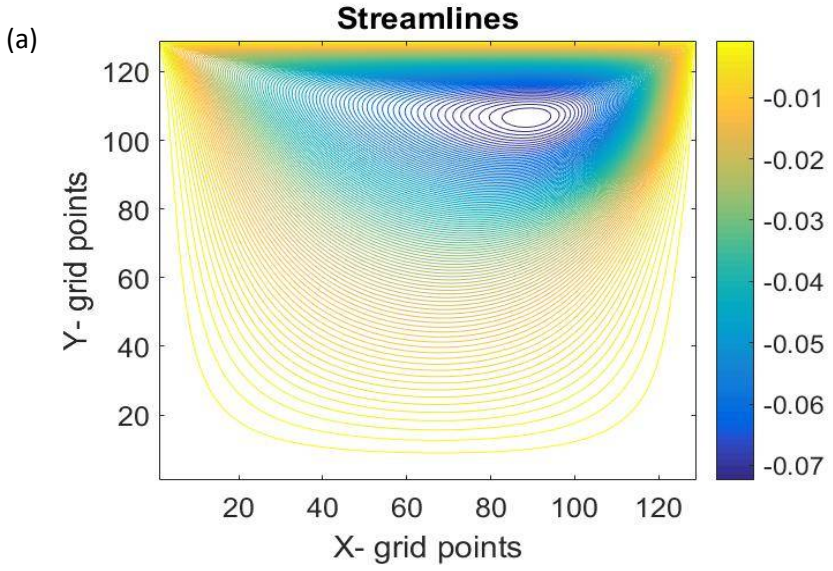

©IJRASET: All Rights are Reserved

(b)

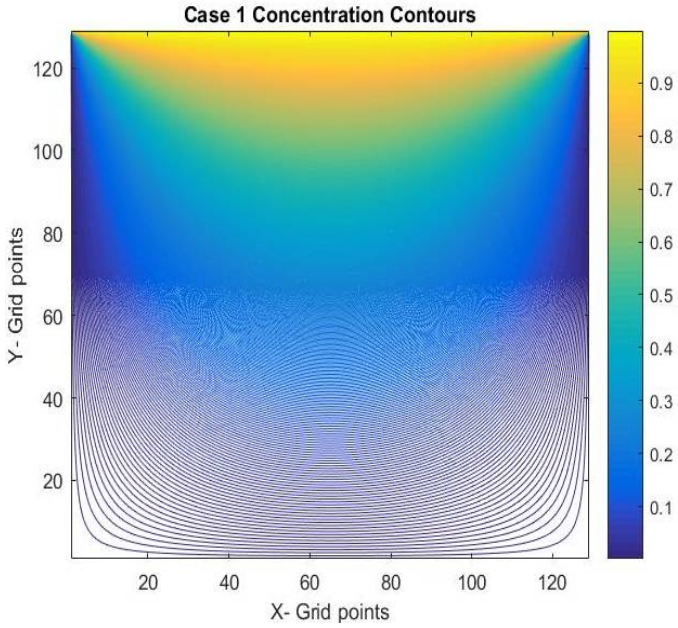

Figure 4.1 Lid driven cavity results (a) Streamlines in lid driven flow (b) Concentration contours

B. Effect of Absorption on Concentration

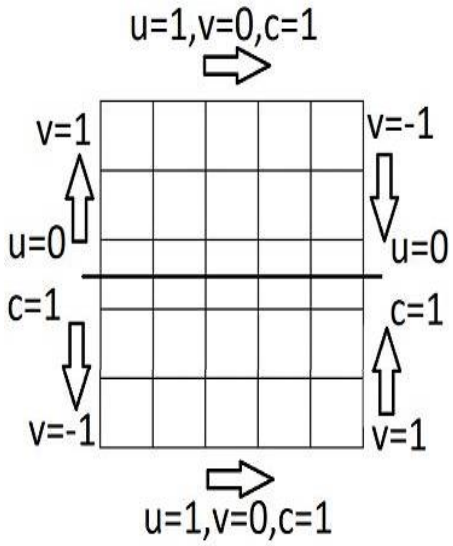

Figure 4.2 Computational Domain for simulating effect of absorption on concentration case

The computational domain for this case is shown in figure 4.2. The problem is solved for the whole physical domain and the effect of varying rate of non-dimensional absorption coefficient is studied. Figure 4.3 shows the stream lines contours. Because of the nature of the problem and the boundary conditions, the fluid from the top half would never mix with the fluid from the bottom half and a kind of solid wall is formed at the centerline. Two separate vortices are formed at each half of the domain and this can be easily seen in figure 4.3.

In figure 4.4 and 4.5, the effect of non-dimensional absorption coefficient can be seen. The concentration contours are similar because absorption is uniform in the domain but the difference can be seen when we look at the colour bar.

©IJRASET: All Rights are Reserved

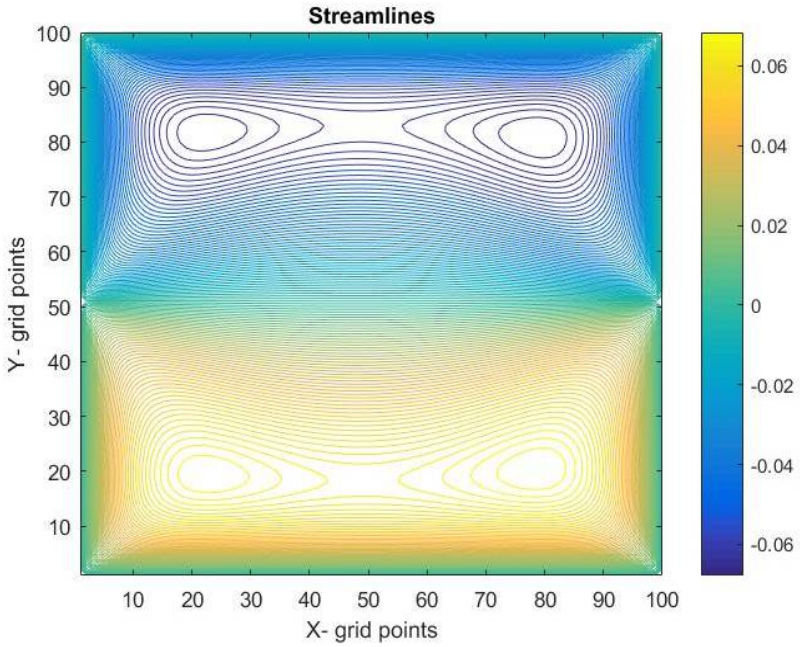

Figure 4.3 Streamline contours for effect of absorption on concentration case

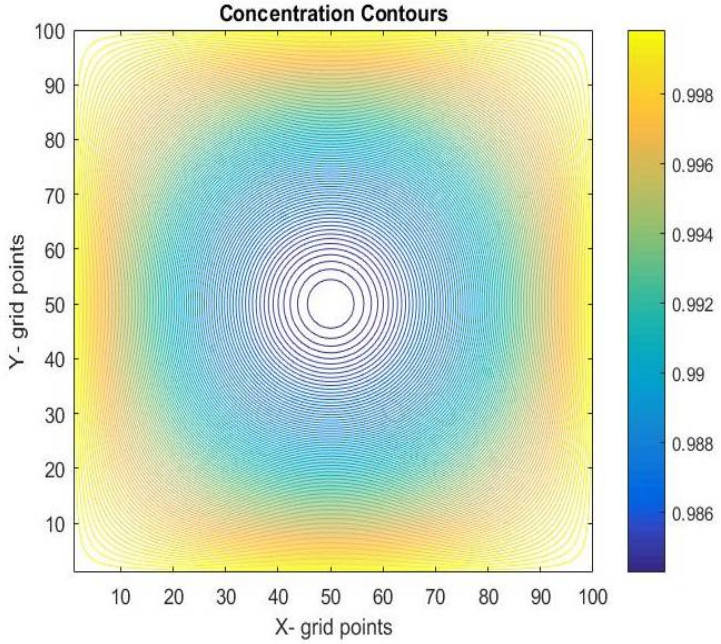

Figure 4.4 Concentration contours (B=1) for effect of absorption on concentration case

Oxygen is diffused from the walls to the center of the domain, so the maximum value of concentration is found at the walls and the minimum value of concentration is found at the center of the domain. When the value of non-dimensional absorption coefficient is 1 the minimum value of concentration is 0.986 and when non-dimensional absorption coefficient is increased to 100, the minimum value of concentration is reduced to 0.92. This decrease in concentration value is because the consumption of oxygen per unit area is increased. This case can be better understood if we consider that when the body is undergoing rigorous physical exercise, the oxygen requirement of the tissues goes up and they try to absorb more oxygen and because of this availability of oxygen in tissue reduces, this is the reason for the decrease of oxygen concentration in tissue as shown in figure 4.5.

©IJRASET: All Rights are Reserved

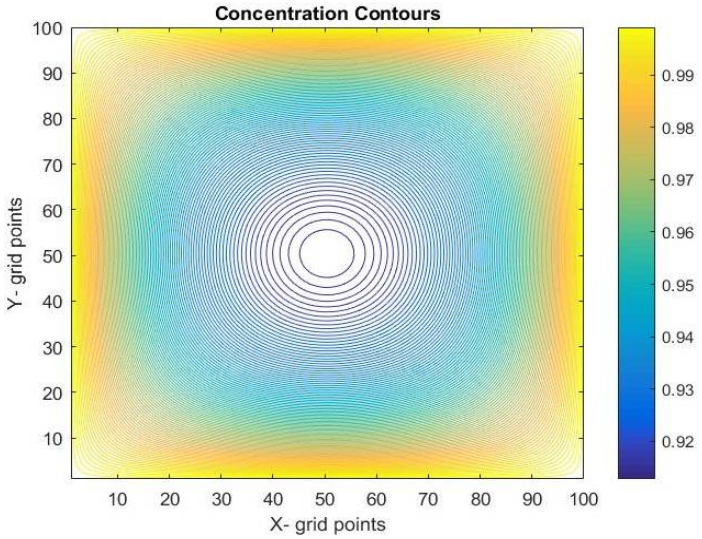

Figure 4.5 Concentration contours (B=100) for effect of absorption on concentration case

C. Transition from Clear Media to Porous Media

This analysis was done to qualitatively study the effect of Darcy number on the transition from clear media to porous media. For the case of clear media Darcy number is infinite (numerically a very large value). In this analysis, Darcy number is reduced from Da=100 to Da=0.001 while all the other parameters are kept constant. A 100×100 grid is used to study the streamline patterns inside the domain. Reynolds number and porosity are 10 and 0.75 respectively.

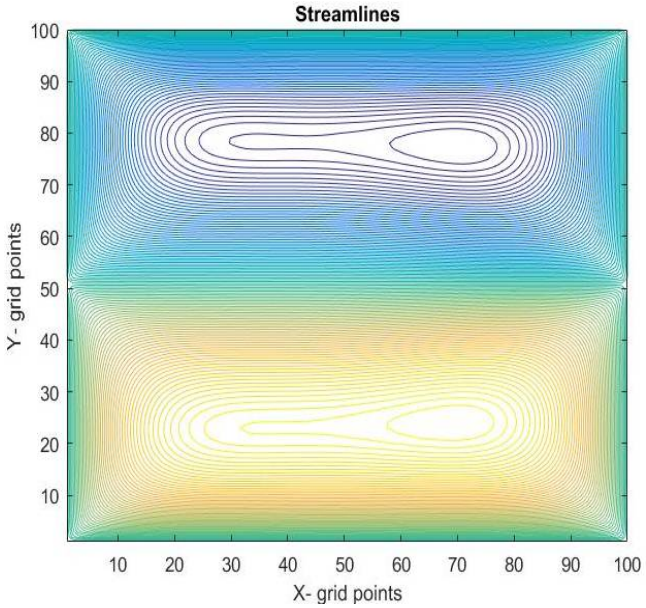

Figure 4.6 Streamline contours (clear media)

In the figure 4.6, streamline is plotted for three cases and it can be seen that there is no difference in the stream line contours between clear media (figure 4.6) and Da= 100 (figure 4.8). In both the plots there are two recirculation zones, one in each of the half. When Darcy number is further reduced to 0.001 (figure 4.7), there is a clear difference in the flow pattern.

©IJRASET: All Rights are Reserved

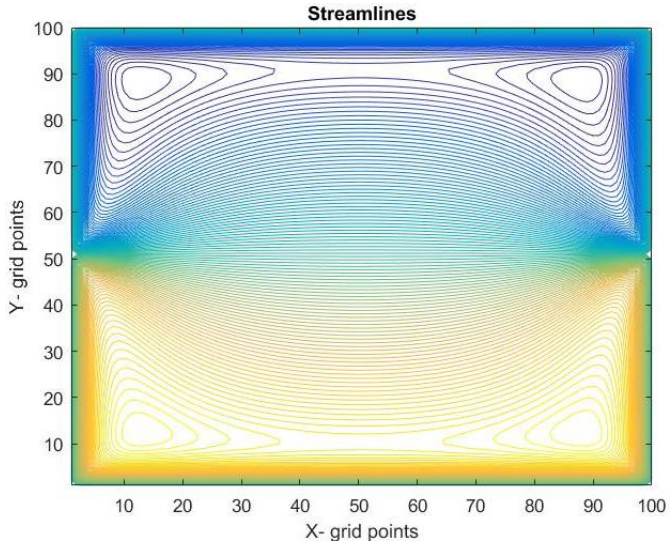

Figure 4.7 Streamline contours (porous media, Da=0.001)

The vortices which were earlier present in the case of clear media and Da=100 have now separated into two vortices each. For the case of Da=0.001, four separate vortices are formed. This is because when we decreased the value of Darcy number to a very small value, the value of permeability is reduced and the effect of the wall was not able to penetrate till the center of the domain and a single recirculation zone in each half could not be formed. Instead two separate recirculation zone had to be formed.

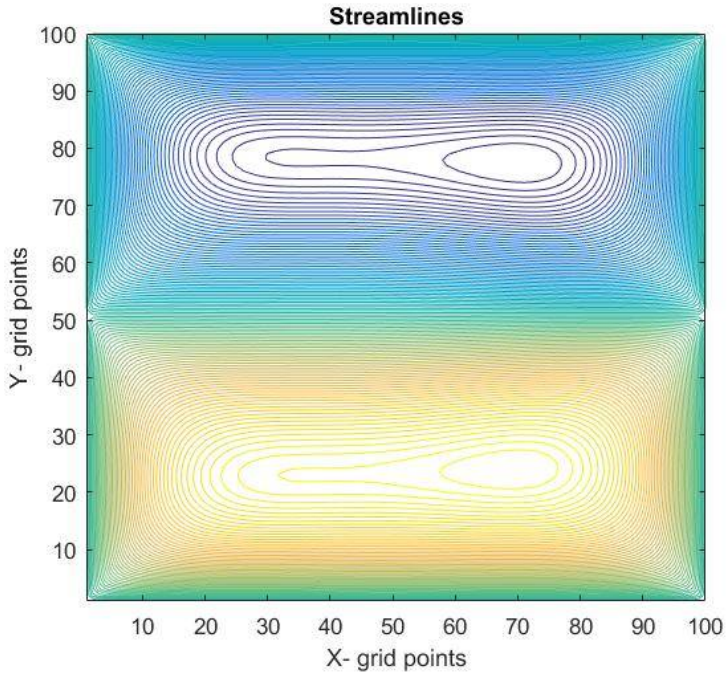

Figure 4.8 Streamline contours (porous media, Da=100)

From this analysis, we could say Da=100 is not small enough to alter flow patterns. Problems in which Darcy number is greater than 100 can be solved treating the porous media as a clear media, if the knowledge of general flow pattern inside a porous media is sufficient. This result could be used as a preliminary study to analyze the flow patterns in a porous media with large Darcy number.

©IJRASET: All Rights are Reserved

V. CONCLUSIONS

In this study, the problem of oxygen transport from blood capillary to tissue is used to study flow and mass transfer in a porous media. A simple but realistic domain has been used treating the tissue as a porous media. The domain is 2-D but it incorporates the effect of interlinkage between blood vessels. Most of the domains available in the literature are either too simple to be realistic or too complicated for a preliminary study such as ours.

Firstly, flow patterns for simple lid driven cavity flow was studied. The effect of porous media killing small vortices and small velocity fluctuation was seen. In lid driven cavity flow for clear media, three vortices are observed but porous media does not allow the smaller vortices to grow, as a result of which only one major vortex is able to form.

Secondly, the effect of non-dimensional absorption coefficient was analysed on the Oxygen concentration contours. It was seen how concentration contours changed when absorption coefficient was increased.

The transition from clear media to porous media was then qualitatively studied by varying Darcy number. The result of this analysis was, we found at Darcy number greater than 100, porous media could be treated as a clear media if the knowledge of general flow pattern is sufficient. This data can then be used for lower Darcy number for faster convergence of results.

REFERENCES

[1] August Krogh. The number and distribution of capillaries in muscles with calculations of the oxygen pressure head necessary for supplying the tissue (1919).
[2] L. Michaelis and Miss Maud L. Menten. The Kinetics of Invertase Action (1913).
[3] Lagerlund TD, Low PA. Axial diffusion and Michaelis-Menten kinetics in oxygen delivery in rat peripheral nerve (1991).
[4] Aleksander S. Popel. Mathematical modeling of oxygen transport near a tissue surface: effect of the surface PO2 (1981).
[5] Daniel A. Beard and James B. Bassingthwaighte. Modeling Advection and Diffusion of Oxygen in Complex Vascular Networks (2001).
[6] Khalil M. Khanafer and Ali J. Chamkha. Mixed convection flow in a lid driven enclosure filled with a fluid saturated porous medium (1998)
[7] U. Ghia, K. N. Ghia, and C. T. Shin. High-Re Solutions for Incompressible Flow Using the Navier-Stokes Equations and a Multigrid Method (1982)
[8] Zhaoli Guo and T. S. Zhao. Lattice Boltzmann model for incompressible flows through porous media (2002).

©IJRASET: All Rights are Reserved

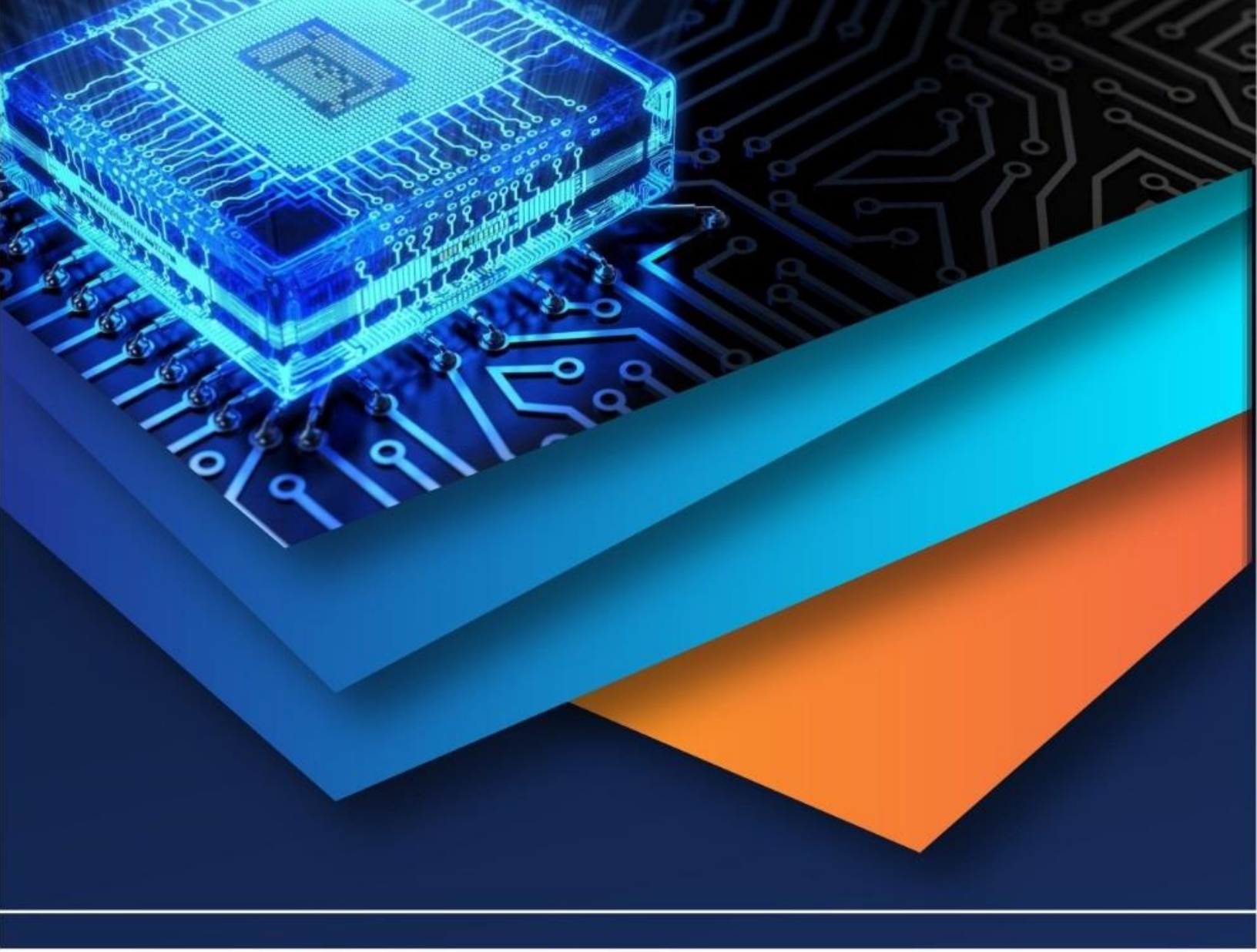

10.22214/IJRASET

45.98

IMPACT FACTOR: 7.129

IMPACT FACTOR: 7.429

INTERNATIONAL JOURNAL FOR RESEARCH

IN APPLIED SCIENCE & ENGINEERING TECHNOLOGY

Call : 08813907089 (24*7 Support on Whatsapp)